Low-temperature thermal conductivity of CaB_6 and EuB_6

2003 J. Phys.: Condens. Matter 15 6739

(http://iopscience.iop.org/0953-8984/15/40/011)

INSTITUTE OF PHYSICS PUBLISHING JOURNAL OF PHYSICS: CONDENSED MATTER

J. Phys.: Condens. Matter **15** (2003) 6739–6748 PII: S0953-8984(03)60099-8

Low-temperature thermal conductivity of CaB_6 and EuB_6

K Giannò[1], A V Sologubenko[1], H R Ott[1], A D Bianchi[2] and Z Fisk[2]

[1] Laboratorium für Festkörperphysik, ETH Hönggerberg, CH-8093 Zürich, Switzerland
[2] National High Magnetic Field Laboratory, Florida State University, 1800 East Paul Dirac Drive, Tallahassee, FL 32306, USA

Received 10 February 2003
Published 26 September 2003
Online at stacks.iop.org/JPhysCM/15/6739

Abstract

The thermal conductivities of stoichiometric CaB_6, vacancy-doped $Ca_{1-\delta}B_6$, and EuB_6 have been measured between 6 and 300 K. All our data may be rather well described across the entire temperature regime covered on the basis of a Debye-type relaxation-time approximation and by assuming the concurring influence of various scattering channels on the mean free path of the phonons. An unusual and strong resonance in the scattering rate of the phonons of all investigated materials is attributed to a strong interaction between acoustic itinerant and localized modes, the latter arising from oscillations of the metal cations around their equilibrium position.

1. Introduction

The search for thermoelectric materials with promising potential for applications is a fascinating subject, since a compound that is considered for practical applications must favourably combine several properties that are related to the electronic structure and transport properties in general. The suitability of a thermoelectric material is quantified by the figure of merit $Z = S^2\sigma/\kappa$, where S is the thermoelectric power, σ the electrical conductivity, and κ the thermal conductivity. In words, for the benefit of practical applications, the thermoelectric power should be high for a good conversion of heat to electrical power or vice versa, whereas the electrical resistivity and the thermal conductivity should both be low in order to minimize Joule heating and thermal shortening, respectively.

Good metals seem favourable because of their high electrical conductivities, but usually they exhibit rather low S-values, of the order of a few microvolts per kelvin. In these cases, the efficient conduction of heat by electrons is also not favourable for keeping the values of Z at a high level. On the other hand, semimetals or degenerate semiconductors exhibit very high S-values but their electrical conductivity is poor. A concentration of itinerant charge carriers of the order of 10^{19} cm^{-3} seems to maximize the quantity $S^2\sigma$ [1]. It has recently been found that materials with conduction electron concentrations of the order of 10^{18} cm^{-3} are found in

the class of hexaborides with divalent cations, such as CaB_6, where at room temperature the thermoelectric power S is of the order of $-300\ \mu V\ K^{-1}$ [2].

For practical applications it is not sufficient that a material has favourable electronic properties: in order to improve the best figure of merit Z, an extraordinarily low thermal conductivity is also required. With regard to this latter prerequisite, a promising category of thermoelectric compounds is provided by materials containing open voids in their crystalline structure, which may be occupied by additional atoms. If the 'guest' atoms are small compared to the size of the void, they will be loosely bound to the rigid cage in which they are embedded, allowing them to 'rattle' around their equilibrium position. The rattling of the guest atoms may result in very low thermal conduction, in some cases even approaching that of the theoretical minimum of the lattice thermal conductivity [3]. The term *clathrates* characterizes a class of solids in which some guest atoms occupy, fully or partially, the voids of cages of the host structures. Clathrates seem well suited for thermoelectric applications because of favourable electronic properties that are associated with this type of material and their drastically reduced thermal conduction.

The radius of the metal cations in the hexaborides mentioned above is significantly smaller than the cell parameter [3, 4], and hence these materials may also be classified as clathrate-type compounds. Here, the role of the guest atoms is played by the metal cations, whereas the host structure is provided by the sublattice of the boron octahedra. Indeed, a resonant scattering of the conduction electrons, leading to a substantial reduction of the thermal conductivity of LaB_6, has been ascribed to the rattling of the loosely bound metal cations in their oversized boron cages [3, 4]. This conclusion is supported by the fact that anomalies in the specific heat data of LaB_6 may successfully be described by treating the La ions as independent Einstein oscillators with an Einstein temperature $\Theta_E = 141$ K [4]. The scattering rate based on the interaction between extended Debye-type modes and the localized Einstein-type lattice excitations has been derived theoretically [5], thus offering the possibility of testing the validity of this model by a corresponding analysis of experimental results of measurements of the thermal conductivity of hexaborides. The frequency of the Einstein mode is expected to decrease with increasing metal cation mass, hence the study of materials with different cations provides an additional test of the conjecture that hexaborides may be classified as clathrate-like compounds.

In this work, we present the results of measurements of the thermal conductivity κ of two CaB_6 samples. One of the samples was prepared in such a way as to obtain material with a close to stoichiometric composition, denoted as CaB_6. The second sample, which we denote as $Ca_{1-\delta}B_6$, is expected to contain a small number of vacancies on the calcium sites, inadvertently introduced during the flux-growth procedure and leading to a certain degree of self-doping which is difficult to control. We also extended the data base on the thermal conductivity of EuB_6, previously presented in [6], to higher temperatures.

This paper is organized as follows. We briefly describe the sample preparation and the experimental set-up in section 2; we then present the results of our measurements and their analysis in section 3. The final section 4 contains a brief summary and some concluding remarks.

2. Samples and experimental method

The single crystals were grown from a melt of nominal composition by a slow-cooling procedure in aluminium flux [7]. The samples for our transport measurements were of prism-type shape with approximate overall dimensions of $4.2 \times 0.5 \times 0.45\ mm^3$ for CaB_6, $4.7 \times 0.45 \times 0.4\ mm^3$ for $Ca_{1-\delta}B_6$, and $1.1 \times 0.21 \times 0.12\ mm^3$ for EuB_6.

We simultaneously measured the thermal conductivity κ and the thermoelectric power S of all samples by means of a standard steady-state heat-flow technique between liquid-helium

and room temperature. Details of our experimental set-up are given in [2], together with results of measurements of the thermoelectric power of the same samples.

In brief, a ^{4}He gas-flow cryostat was used to cool the materials under investigation. By using high-conductance silver epoxy, good thermal contact to a heat sink made of copper was ensured at one end of the prism-shaped samples. On the other end of the prisms, a 100 Ω ruthenium-oxide chip resistor was attached by using the same glue. Joule heating caused by heater currents of the order of a few milliamperes provided the necessary heat-flow and hence a thermal gradient along the crystals. The temperature difference ΔT between two contacts mounted perpendicularly to the heat flow was measured by using two pairs of calibrated Au–Fe (0.07 at.%) versus chromel thermocouples [8]. The advantage of this choice, compared to the usage of resistance thermometers, is that thermocouples have a much smaller surface, resulting in a substantial reduction of thermal radiative losses. Very thin (25 μm in diameter) and long (up to 10 cm) wires have been chosen in order to reduce the heat flow through the thermocouples.

Thermal-conductivity measurements of materials with low thermal-conductivity values are generally difficult to perform at high temperatures because of the detrimental effect of radiative losses on the results. In order to limit this kind of energy dissipation, a cylindrical radiation shield in good thermal contact with the heat sink was installed. By using similar arguments to those presented in [8], the radiative losses in our measurements have been estimated to be below 0.5% of the applied power over the whole temperature range

3. Experimental results and analysis

In figure 1, we display the measured thermal conductivities $\kappa_{\rm meas}$ of CaB_6, $Ca_{1-\delta}B_6$, and EuB_6 on logarithmic scales between 6 and 300 K. In the following analysis we assume that only conduction-electron and lattice contributions to $\kappa_{\rm meas}$ need to be considered.

The electronic contributions to the thermal conductivities of CaB_6 and $Ca_{1-\delta}B_6$, shown in figure 1 as solid curves, were calculated by using the Wiedemann–Franz relation $\kappa_{\rm el} = L^*\sigma T$, with L^* for CaB_6 and $Ca_{1-\delta}B_6$ as calculated in [2]. The electrical conductivities σ utilized for the calculation of the electronic contribution to the thermal conductivity were measured on the same samples by using a four-point low-frequency technique. The electrical resistivities $\rho = 1/\sigma$ of all samples investigated here are presented in figure 2 between 5 and 300 K. For the benefit of the reader, a plot of the calculated L^* between 5 and 300 K is presented in figure 3. For EuB_6, L^* was assumed to be the classical Lorenz number. For all materials, the estimated $\kappa_{\rm el}$ is at least two orders of magnitude smaller than $\kappa_{\rm meas}$ at all temperatures covered in this study. Since the experimental uncertainty in our measurements of the thermal conductance is of the order of 0.5%, the procedure for estimating $\kappa_{\rm el}$ is not critical and may be considered as sufficiently accurate for the validity of the following considerations.

The lattice contributions $\kappa_{\rm ph} = \kappa_{\rm meas} - \kappa_{\rm el}$ to the thermal conductivities of all samples are shown in figure 4, revealing monotonic increases of $\kappa_{\rm ph}$ with T up to 18 K for CaB_6 and EuB_6, and 23 K for $Ca_{1-\delta}B_6$, respectively. At these temperatures, $\kappa_{\rm ph}$ passes over maxima of 124 and 99 W m^{-1} K^{-1} for CaB_6 and EuB_6, respectively, and 74 W m^{-1} K^{-1} for $Ca_{1-\delta}B_6$, and subsequently decreases with varying slopes up to room temperature. We note that at low temperatures $\kappa_{\rm ph}$ of $Ca_{1-\delta}B_6$ adopts distinctly lower values than $\kappa_{\rm ph}$ for CaB_6. This seems reasonable because of the expected enhanced scattering of the phonons by defects in the Ca-deficient material. The crossing of the two curves at a temperature close to 30 K is, however, rather surprising and implies a much more efficient high-frequency scattering mechanism for phonons in the structurally more perfect sample.

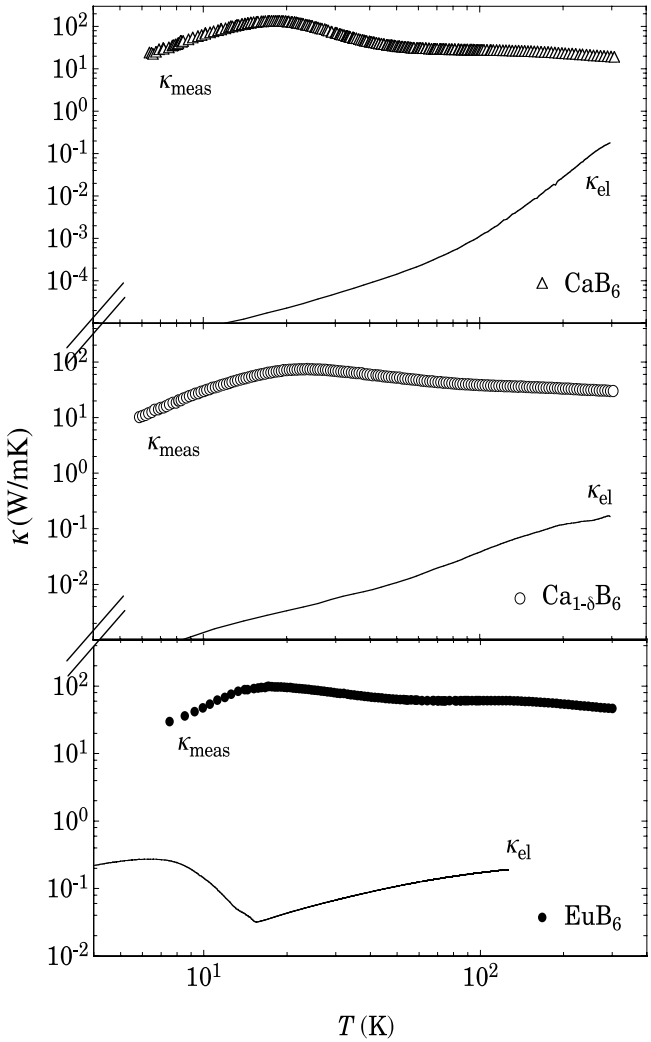

Figure 1. The measured thermal conductivities κ_{meas} of CaB_6, $Ca_{1-\delta}B_6$, and EuB_6 and their calculated electronic contributions κ_{el} (see text) as a function of temperature on logarithmic scales.

The following quantitative analysis of our data is based on a relaxation-time approximation combined with the Debye model. The Debye approximation is strictly only valid at temperatures which are low enough with respect to the Debye temperature Θ_D. In this way we assume that only the modes of the acoustic branches $\omega(k)$ that are well approximated by a linear k dependence contribute to κ_{ph}. Since the temperature range covered in our experiment is considerably lower than the Debye temperatures of $\Theta_D = 783$ K for CaB_6 [9] and $\Theta_D = 570$ K for EuB_6 [6], this approximation is justified, at least to some extent. The thermal conductivity may thus be calculated from

$$\kappa_{ph}^{fit} = 3nk_B\left(\frac{T}{\Theta_D}\right)^3 v_{ph}^2 \int_0^{\Theta_D/T} \frac{x^4 e^x}{(e^x-1)^2}\tau(x,T)\,dx, \tag{1}$$

where $\tau(x, T)$ is the average time between collisions of a phonon, n is the number density of atoms in the crystal, and $x = \hbar\omega/k_B T$. For the Debye temperatures Θ_D, we used the above

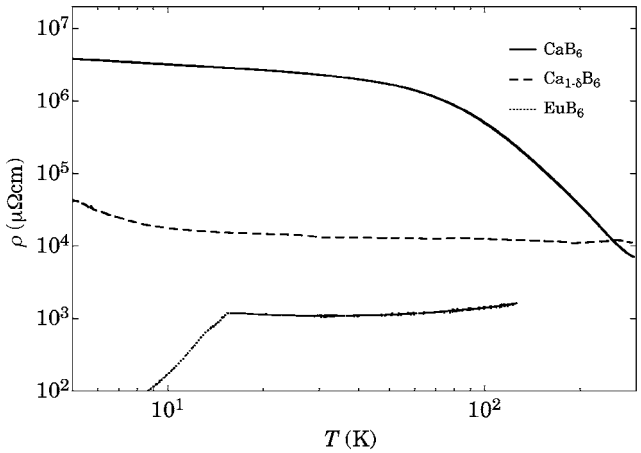

Figure 2. Electrical resistivities of CaB_6, $Ca_{1-\delta}B_6$, and EuB_6 as a function of temperature between 5 and 300 K.

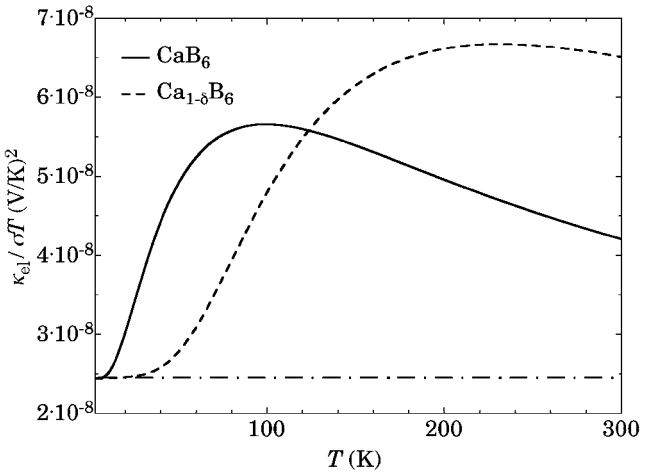

Figure 3. Ratio $\kappa_{el}/\sigma T$ for CaB_6 and $Ca_{1-\delta}B_6$ as a function of temperature between 5 and 300 K, from [2]. The horizontal dashed–dotted curve represents the temperature independent Lorenz number $L_0 = 2.45 \times 10^{-8}$ V^2 K^{-2}.

cited values, which were either extracted from specific-heat measurements on stoichiometric CaB_6 [9] or estimated as described in [6] for EuB_6. Since, upon introducing a very small number of calcium vacancies, no significant changes in the lattice contribution to the specific heat are expected, we used the same Debye temperature for CaB_6 and $Ca_{1-\delta}B_6$. This argument is supported by the observation that no significant differences between the low-temperature specific heats of CaB_6 and $Ca_{1-x}La_xB_6$ with $x = 0.005$ were identified [9]. The number density of atoms can be calculated from the lattice constants $a = 4.146$ and 4.185 Å for CaB_6 and EuB_6 [10, 11]. From the relation

$$n = 1/6\pi^2(k_B\Theta_D/\hbar v_{ph})^3, \tag{2}$$

we may also calculate the average velocity of the vibrational modes for which we obtained $v_{ph} = 5722$ and 4205 m s^{-1} for CaB_6 and EuB_6, respectively.

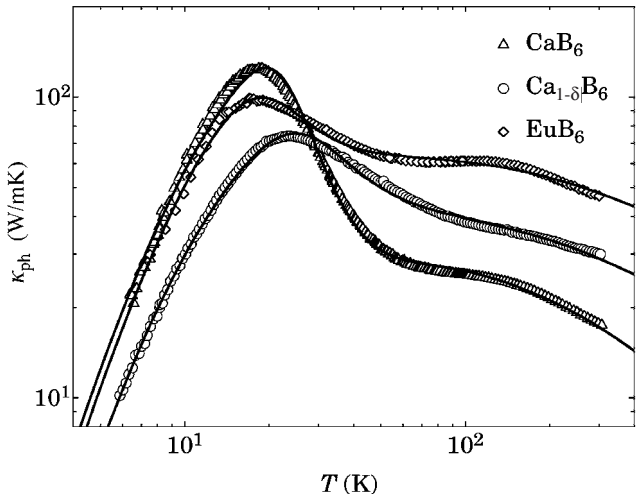

Figure 4. The lattice contributions to the thermal conductivities κ_{ph} of CaB_6, $Ca_{1-\delta}B_6$, and EuB_6 as a function of temperature on logarithmic scales. The solid curves correspond to fits to the data as explained in the text.

Table 1. Parameters provided by the fitting of the $\kappa_{ph}(T)$-data to equations (1) and (3).

Fit parameter	CaB_6	$Ca_{1-\delta}B_6$	EuB_6
l_{Cas} (μm)	92.5 ± 0.2	52.5 ± 0.1	42.7 ± 0.3
A (10^{-44} s^3)	6.00 ± 0.02	13.61 ± 0.05	8.4 ± 0.1
B (10^{-15} s)	7 ± 1	1.5 ± 0.2	3 ± 1
C (10^{-19} s K^{-1})	10.6 ± 0.2	1.58 ± 0.05	0.41 ± 0.02
α (10^9 m^{-1})	9 ± 2	9 ± 1	14 ± 5
ω_s (10^{13} s^{-1})	2.876 ± 0.001	2.610 ± 0.005	2.011 ± 0.003
$\hbar\omega_s/2k_B$ (K)	109.41 ± 0.04	99.3 ± 0.2	76.5 ± 0.1

For the evaluation of the integral in equation (1), we approximated the phonon relaxation rate by

$$\tau^{-1}(x, T) = \tau_{Cas}^{-1} + \tau_{Rayl}^{-1}(x, T) + \tau_{res}^{-1}(x, T) + \tau_{U}^{-1}(x, T). \tag{3}$$

The different terms on the right-hand side of equation (3) represent the scattering of phonons at grain or sample boundaries, by point defects, via resonant scattering, and due to phonon–phonon umklapp processes. The resulting fits are shown in figure 4 as solid curves. In what follows, we discuss each term appearing in equation (3) separately. The values of the free parameters involved in our fitting procedure (see below) are given in table 1.

The temperature- and frequency-independent scattering length l_{Cas}, related as $\tau_{Cas}^{-1} = v_{ph}/l_{Cas}$, is the so-called Casimir length, where the phonon mean free path is limited by sample boundaries [12]. The values between 0.043 and 0.093 mm shown in table 1 are close to the order of magnitude of the smallest sample dimensions, considering the variation of the sample cross section perpendicular to the direction of the thermal current.

The enhanced number of scattering centres at the vacancy sites in $Ca_{1-\delta}B_6$ is unequivocally reflected in the second term of equation (3). In the continuum approximation, Rayleigh

scattering by pointlike mass defects leads to a scattering rate term $\tau_{\mathrm{Rayl}}^{-1} = A\omega^4$, with [13]

$$A = \frac{n_{\mathrm{p}} a^6}{4\pi v_{\mathrm{ph}}^3} \left(\frac{\delta M}{M} \right)^2 . \tag{4}$$

In equation (4), n_{p} is the number density of point defects, a is the lattice constant, M is the mass of a unit cell, and δM is the excess or missing mass due to a point defect in a sphere with the radius of the point defect itself. Since the extra mass term appears squared in equation (4), it is not possible to decide whether δM is positive or negative. The parameter A resulting from the best fit to the $Ca_{1-\delta}B_6$ data is approximately twice as large as the corresponding value for CaB_6. The same ratio is reflected in the number of itinerant charge carriers in either $Ca_{1-\delta}B_6$ or CaB_6, as established in [2].

For this reason, we now assume that the mass defects are due to calcium vacancies in both compounds, leading to a $\delta M/M$ value of 0.38. Based on this assumption, the fit values of A listed in table 1 imply point-defect density values n_{p} of 1.9 and 4.3×10^{20} cm^{-3} for CaB_6 and $Ca_{1-\delta}B_6$, corresponding to 170 and 140 times the charge carrier densities in the same materials [2]. We interpret this result as follows. The vacancies of Ca^{2+} ions in the lattice are responsible for the formation of a defect band in the charge-carrier excitation spectrum. A small number of these charge carriers are transferred to the conduction band and hence become mobile. It must be kept in mind, however, that equation (4) merely indicates the presence of mass defects in the lattice and does not contain any information regarding the nature of the defects. A similar interpretation may be given by assuming the presence of impurities in the investigated samples, others than those considered in this work.

Resonant scattering of phonons had to be invoked in the analysis of the thermal conductivity data of EuB_6 in a previous report [6]. The resonant scattering of phonons in EuB_6 was intepreted as being due to a resonant scattering of low-momentum itinerant vibrational states in the low-frequency part of the $\omega(k)$ branches with acoustic modes of constant energy that seem to occupy an extended region of the Brillouin zone at higher momenta. Indeed, a rapid flattening of the LA branches at an energy of approximately 12 meV was observed in inelastic neutron scattering experiments performed on hexaborides XB_6 with trivalent cations X = Ce, La, Sm [14–16]. The rapid flattening of the acoustic branches in LaB_6 was later ascribed to the strong interaction between a localized Einstein mode at an energy of approximately 12 meV, corresponding to an Einstein temperature $\Theta_{\mathrm{E}} = 140$ K, and the itinerant acoustic phonons [3, 4]. The lanthanum ions are thought to be loosely bound in a rigid cage made of covalently connected boron octahedra [4]. Since the available space around the lanthanum atoms is much larger than the size of the atom itself [4], the metallic ion is allowed to oscillate rather freely around its equilibrium position. By treating the La atoms as Einstein oscillators embedded in a boron network which can be described as a Debye solid, the authors of [4]. were also able to reproduce the temperature dependences of the measured electrical resistivity and specific heat of LaB_6.

A calculation of the resonant relaxation time of the lattice vibrations, based on an atomistic model which describes the inelastic phonon scattering processes in the presence of localized modes, was given by Wagner [5], following the experimental results presented by Walker and Pohl [17]. In this approximation, the corresponding phonon relaxation rate is expressed as

$$\tau_{\mathrm{res}}^{-1} = B f(\omega, T) g(\omega), \tag{5}$$

with

$$B = \frac{9}{16} \frac{\pi^2}{\rho} \frac{\gamma^2 \hbar}{v_{\mathrm{ph}}} \frac{(Z\alpha) n_{\mathrm{res}}}{\omega_{\mathrm{s}}}, \tag{6}$$

$$f(\omega, T) = \frac{(\omega_s - \omega)^2 e^{\hbar(\omega_s-\omega)/k_B T}(e^{\hbar\omega/k_B T} - 1)}{(e^{\hbar\omega/k_B T} - 1)(e^{\hbar(\omega_s-\omega)/k_B T} - 1)}, \tag{7}$$

and

$$g(\omega) = \left(1 + 4\frac{\omega_\alpha}{\omega_s}\right) \ln\left\{\frac{(\omega/\omega_s)(1 - (\omega/\omega_s)) + (\omega_\alpha/\omega_s)}{\omega_\alpha/\omega_s}\right\} - 4\frac{\omega}{\omega_s}\left(1 - \frac{\omega}{\omega_s}\right). \tag{8}$$

Here ρ is the material's mass density, γ the lattice Grüneisen constant, Z the number of localized modes per resonator, α the exponential damping coefficient of the localized mode, n_{res} the concentration of resonators, ω_s the frequency of the stationary modes, and $\omega_\alpha = \alpha v_{ph}$. The remaining parameters are the same as defined above. It turns out that the quoted resonant term suggested by Wagner [5] is the only, physically justified, scattering rate which allows for a description of all our data sets. Below we briefly discuss the parameters in equation (5) which were evaluated via the fitting procedure, i.e., Zn_{res}, α, and ω_s.

Employing equation (6) and inserting the fit values listed in table 1, the number of localized modes per unit cell Zn_{res}, expressed in units of $(2/\gamma)^2$, is 10 ± 3 for CaB_6, 1.9 ± 0.3 for $Ca_{1-\delta}B_6$, and 3 ± 1 for EuB_6. Although not exactly, these values are all of order unity, indicating that every cubic unit cell in the investigated hexaborides indeed contains one resonator which we interpret as being the metal cation located at the centre of the cell. With this intepretation of the data, the crossing of the thermal conductivity curves of the two Ca based hexaborides at $T = 30$ K points to a much stronger resonant scattering rate in CaB_6. The best fit value for Zn_{res} for CaB_6 is approximately a factor of three larger than the one observed in the other two investigated materials. The physical reason for this unexpected observation could not be identified in this investigation.

The high values of the damping factor α resulting from our best fits are also listed in table 1. They indicate that the oscillations die off on short distances. The amplitude of a metal–cation vibration vanishes within a lattice constant a to less than its eth part, supporting the quoted assumption that the modes are localized.

The values ω_{res} of the calcium compounds are about 40% higher than the one derived for the europium-based hexaboride. A higher Einstein frequency for a lighter cation is indeed expected. In the case of a harmonic potential, for instance, the oscillation frequency is expected to scale with the inverse of the square root of the cation's mass, whereas an inverse mass proportionality of the frequency is encountered for a rectangular quantum well with impermeable walls. Since we do not know the exact form of the electrostatic potential around the metal cation of hexaborides, we are not in a position to test whether the encountered difference in resonant frequency is entirely due to the mass difference between Eu and Ca, or whether an additional mechanism, e.g., a different coupling strength between the metal cations and the rest of the lattice, should be taken into account.

The last term in the scattering rate appearing in equation (3) provokes the enhanced negative slope of $\kappa_{ph}(T)$ above approximately 150 K for CaB_6 and EuB_6 (see figure 4). For this term, describing an umklapp type of phonon scattering, we used [18]

$$\tau_U^{-1} = CT\omega^2 \exp\left(-\frac{\Theta_D}{bT}\right). \tag{9}$$

In order to limit the number of free parameters in our fitting procedure, we fixed the value of b in equation (9) to $b = 2\sqrt[3]{7}$, where 7 is the number of atoms per unit cell. The exponential decay of $\kappa_{ph}(T)$ dictated by equation (9), usually observed in crystals of high structural quality in the temperature range [18] $1/30 < T/\Theta_D < 1/10$, cannot be observed here, because the scattering of the phonons at these temperatures is dominated by the resonant type of scattering discussed above.

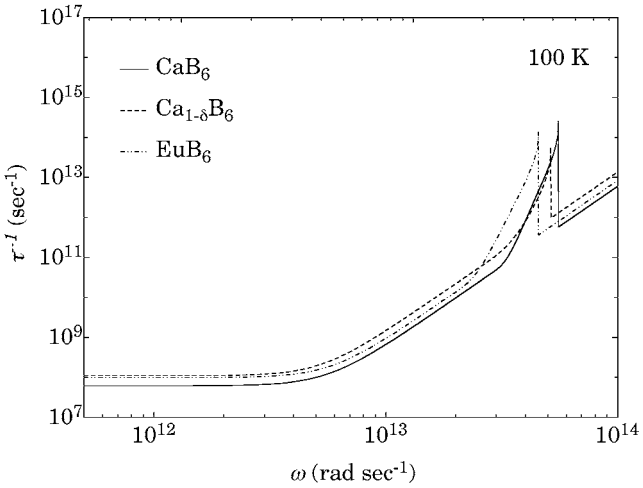

Figure 5. The total phonon relaxation rate τ^{-1} resulting from our fit (see equation (3)) as a function of frequency for $T = 100$ K.

As an example, the resulting total scattering rate of the phonons as a function of frequency is shown in figure 5 for $T = 100$ K. In this graph, the influence of the resonant type of scattering on the total scattering rate of the phonons is clearly manifest at frequencies around $2\omega_s$.

In the introductory section, we expressed our interest in the thermal conductivity of hexaborides by mentioning the feasibility of using clathrates for thermoelectric applications. Therefore it seems appropriate to briefly discuss the usefulness of the investigated materials for thermoelectric applications. The dimensionless figure of merit $ZT = S^2\sigma T/\kappa$ of close to stoichiometric CaB_6, the material with the highest ZT value investigated in this context, is about 0.02 at room-temperature. This is approximately a factor 50 lower than what is reached for state-of-the-art thermoelectric materials. A much improved figure of merit may, nevertheless, be expected for CaB_6 at temperatures exceeding 300 K. While the thermoelectric power S is still increasing with T at room temperature [2], the slopes of the temperature dependence of the electrical resistivity $\partial\rho/\partial T$ [9] and the thermal conductivity $\partial\kappa/\partial T$ are both negative and, hence, a rapid improvement of ZT with increasing temperature may be anticipated.

Some general considerations serve to support this optimistic conjecture. In particular, in view of the Debye temperature Θ_D of CaB_6 of 783 K, an enhanced influence of the umklapp processes will limit κ_{ph} at temperatures above $\Theta_D/2 \approx 400$ K [18]. Moreover, the mass-defect induced scattering of the vibrational modes, as shown in equation (4), can be further enhanced by isovalent substitutions of the boron atoms. Because of the small weight of the boron atoms, this should be of great impact, if we consider the term $\delta M/M$ in equation (4). The distance between the scattering centres is of the order of $1/n_p^{1/3} \sim 15$ Å. The wavelength $\lambda_F = 2\pi/k_F \sim 100$–$200$ Å of the electrons at the Fermi energy is one order of magnitude larger than the wavelength $2\pi v_{ph}/\omega_s \sim 10$–$20$ Å of the phonons just below the resonance. Since the electrons have a wavelength longer than the distance between the scattering centres, they will be less scattered by the enhanced mass fluctuations than the phonons, and hence the electrical conductivity should not be affected in the same drastic manner.

CaB_6 is obviously not a serious rival for other materials in thermoelectric applications below room temperature. However, based on our understanding of the electrical and thermal transport properties below 300 K, we expect a significant increase of the ZT values for this

compound above room temperature. Since all five parameters contributing to ZT (by counting S twice as it appears squared in ZT) are developing in a favourable direction above room temperature, it is quite likely that CaB_6 is a competitive thermoelectric material at temperatures T exceeding 300 K.

4. Summary and conclusion

We have measured the thermal conductivity of close to stoichiometric CaB_6, vacancy-doped CaB_6, and EuB_6 between 6 and 300 K. A Debye-type relaxation-time approximation is successful in describing the thermal conductivity data across the entire temperature range covered in the experiments. We have shown that the usual terms contributing to the total scattering rate of the vibrational states, i.e. the Casimir- and the Rayleigh-scattering terms, are consistent with some reasonable expectations. A rather unusual temperature dependence of κ_{ph} is observed above approximately 30 K. A resonant type of scattering seems to influence the mean free path of the phonons at these temperatures. Quite surprisingly, its limiting effect on the time period between two vibrational-mode collisions is much stronger in the material with fewer defects. According to theoretical expectations, the resonant scattering is related to inelastic scattering processes of the phonons in the presence of localized modes. We attribute the presence of these localized modes to the peculiar structure of hexaborides, which allows the metal cations located at the centre of an oversized unit cell to move freely around their equilibrium positions. Finally, we ascribe the enhanced decrease of the thermal conductivity at higher temperatures to structural or umklapp scattering.

Acknowledgments

We thank R Monnier for stimulating discussions. This work was financially supported by the Schweizerische Nationalfonds zur Förderung der Wissenschaftlichen Forschung.

References

[1] Ioffe A F 1957 *Semiconductor Thermoelements and Thermoelectric Cooling* (London: Infosearch)
[2] Giannò K, Sologubenko A V, Ott H R, Bianchi A D and Fisk Z 2002 *J. Phys.: Condens. Matter* **14** 1035
[3] Sales B C, Mandrus D G and Chakoumakos B C 2001 *Semicond. Semimet.* **70** 1
[4] Mandrus D G, Sales B C and Jin R 2001 *Phys. Rev.* B **64** 012302
[5] Wagner M 1963 *Phys. Rev.* **131** 1443
[6] Vonlanthen P, Paschen S, Pushin D, Bianchi A D, Ott H R, Sarrao J L and Fisk Z 2000 *Phys. Rev.* B **62** 3246
[7] Fisk Z and Remeika J P 1989 Growth of single crystals from molten metal fluxes *Handbook on the Physics and Chemistry of Rare Earths* vol 12, ed K A Gschneider and L Eyring (New York: Elsevier) pp 53–71
[8] Bougrine H and Ausloos M 1995 *Rev. Sci. Instrum.* **66** 199
[9] Vonlanthen P, Felder E, Degiorgi L, Ott H R, Young D P, Bianchi A D and Fisk Z 2000 *Phys. Rev.* B **62** 10076
[10] Naslain R, Etourneau J and Hagenmueller P 1977 *Boron and Refractory Borides* ed V I Matkovich (Berlin: Springer) p 262
[11] Süllow S, Prasad I, Aronson M C, Sarrao J L, Fisk Z, Hristova D, Lacerda A H, Hundley M F, Vigilante A and Gibbs D 1998 *Phys. Rev.* B **57** 5860
[12] Casimir H B G 1938 *Physica* **5** 495
[13] Ziman J M 1960 *Electrons and Phonons* (London: Oxford University Press)
[14] Alekseev P A, Ivanov A S, Dorner B, Schober H, Kikoin K A, Mishchenko A S, Lazukov V N, Konovalova E S, Paderno Y B, Rumyantsev A Y and Sadikov I P 1989 *Europhys. Lett.* **10** 457
[15] Kunii S, Effantin J M and Rossat-Mignod J 1997 *J. Phys. Soc. Japan* **66** 1029
[16] Smith H G, Dolling G, Kunii S, Kasaya M, Liu B, Takegahara K, Kasuya T and Goto T 1985 *Solid State Commun.* **53** 15
[17] Walker C T and Pohl R O 1963 *Phys. Rev.* **131** 1433
[18] Berman R 1976 *Thermal Conduction in Solids* (Oxford: Oxford University Press) p 57